

Investigation of the Structural Variation after the Intercalation of Cetylpyridinium Chloride into V_2O_5 Xerogel

Elidia Maria Guerra*, Dane Tadeu Cestaroli*, Herenilton Paulino Oliveira**

*(Department of Chemistry, Biotechnology and Bioprocess Engineering, Federal University of São João Del Rei, Brazil)

** (Department of Chemistry, São Paulo University, Brazil)

ABSTRACT

A new hybrid material using vanadium pentoxide xerogel in different concentration of the cationic surfactant cetylpyridinium chloride (V_2O_5 CPC) is investigated. The insertion was accompanied by XRD, FTIR and SEM characterization. These studies revealed the presence of a lamellar structure for the V_2O_5 CPC hybrid material in all concentrations of cetylpyridinium chloride. The intercalation reaction was evidenced on basis of the increase in the d-spacing as well as the displacement of the infrared bands toward lower energy levels. The CPC intercalation occurred by reorganize intermittently forming two domains within the matrix.

Keywords– Cetylpyridinium chloride; hybrid materials; intercalation; sol-gel; V_2O_5

I. INTRODUCTION

Layered inorganic–organic hybrid materials have received a lot of research interest because of their combined inorganic–organic feature which has tailored applications in catalysis, adsorption, and separation process [1,2]. Besides, the expandability between the interlayer spaces provides a good place for studying guest–host interaction between the inserted organic molecules attached on the inorganic layers [3-6]. In particular, vanadium based oxides have attracted considerable attention not only because of the structural versatility [7-9] of vanadium but also due to their ability to act as intercalation [10], ion-exchange [11], sorption [12], magnetic [13] and as cathodic material [14]. Concerning to the use as cathodes batteries, the lamellar structure of V_2O_5 matrix allows Li^+ intercalation/deintercalation during the reduction/oxidation of vanadium cations [15,16].

Furthermore, based on cooperative assembly of molecular V_2O_5 matrix/surfactant species [17] the charge density of the inorganic species determines how many surfactant molecules are associated with a given inorganic molecular unit as well as the preferred orientation of the surfactant head group relative to the molecular inorganic species [18]. The formation of the hybrid compound matrix/surfactant, such as V_2O_5 /cetylpyridinium chloride, could be related to the presence of the negatively charged inorganic species interacted with the positively charged ammonium headgroups of the surfactant due to electrostatic interaction and condensed into a solid, continuous framework [19].

The purpose of the present study is to investigate the structural variation in response of the thermal treatment after the intercalation of CPC into V_2O_5

xerogel and the structure of host-guest composite at the early stage as accomplishment of a steady state of intercalation.

II. MATERIALS AND METHODS

2.1. Reagents

Cetylpyridinium chloride was purchased from Acros. Acetonitrile was chromatographic grade (Fluka), the vanadium pentoxide xerogel was prepared from sodium metavanadate (Fluka), and the ion-exchange resin was Dowex-50X8 in its acid form. Water was purified using a Millipore Milli-Q System.

2.2. Equipment and procedure

The X-ray diffraction (XRD) data were recorded on a SIEMENS D5005 diffractometer using a graphite monochromator and CuK α emission lines (1.541 Å, 40 kV, 40 mA). To this end, samples in the film form and deposited onto a glass plate were employed, and the data were collected at room temperature over the range $2^\circ \leq 2\theta \leq 50^\circ$, with a step of 0.020° . Fourier-transform infrared spectra (FTIR) were recorded from 4000 to 400 cm^{-1} on a Bomem MB 100 spectrometer, and the samples were dispersed in KBr and pressed into pellets. Scanning electronic microscopy (SEM) studies were carried out on a ZEISS-DSM 940 microscope operating at 20 kV.

2.3. Preparation of the V_2O_5 /CPC hybrid material

Initially, in 5 mL the V_2O_5 xerogel in 0.1 dm^{-3} were added different concentrations of CPC at room temperature under constant stirring for 48 h [20]. The resulting brown suspension was cast into a film form by evaporation of water at room

temperature on a glass. Afterward, the resulting film was rinsed with deionized water and dried again at room temperature. The color of the film was light brown with metallic luster. The samples were named as follows:

CPC (mmol dm ⁻³)	Composite name in 5 mL of 0.1 mol.dm ⁻³ of V ₂ O ₅
1	V ₂ O ₅ CPC1
2	V ₂ O ₅ CPC2
3	V ₂ O ₅ CPC3
20	V ₂ O ₅ CPC20
40	V ₂ O ₅ CPC40
60	V ₂ O ₅ CPC60
80	V ₂ O ₅ CPC80
100	V ₂ O ₅ CPC100

III. RESULTS AND DISCUSSIONS

Figure 1(a-i) shows the diffractograms of vanadium pentoxide xerogel and the composites V₂O₅CPC1, V₂O₅CPC2, V₂O₅CPC3, V₂O₅CPC20, V₂O₅CPC40, V₂O₅CPC60, V₂O₅CPC80 and V₂O₅CPC100, respectively.

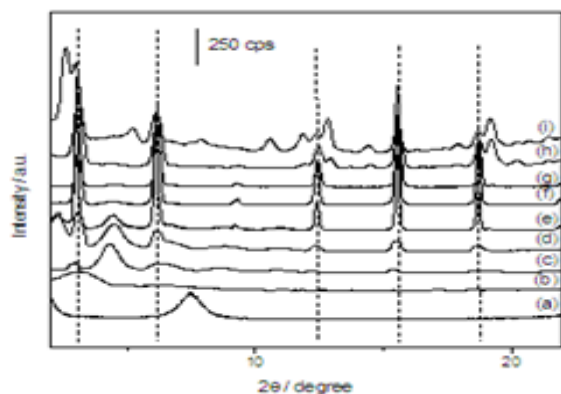


Fig. 1 X-Ray diffraction of (a) V₂O₅.nH₂O xerogel and of composites of (b) V₂O₅CPC1, (c) V₂O₅CPC2, (d) V₂O₅CPC3, (e) V₂O₅CPC20, (f) V₂O₅CPC40, (g) V₂O₅CPC60, (h) V₂O₅CPC80 and (i) V₂O₅CPC100.

It was observed in diffractograms of the composites diffraction peaks (00l) indicating that the lamellar structure of V₂O₅ was preserved, which is consistent with a topotactic process. Besides, was observed, after intercalation of CPC, a interlayer increase, Δd, compared to V₂O₅ that presents a interlayer distance of 11,70 Å. Probably, this increase in d-spacing is an evidence of the CPC insertion into the matrix. The Δd values are showed in Table 1.

Table 1 Values of the interlayer distances (d), variation of the interlayer distances of the composite V₂O₅CPC in different concentration of surfactant.

Composites	Values of d ₀₀₁ (Å)	Δd (Å)	Inclination angle (θ)
V ₂ O ₅ CPC1	28.50	16.80	40°
V ₂ O ₅ CPC2	30.40	18.70	47°
V ₂ O ₅ CPC3	40.10	28.40	-
V ₂ O ₅ CPC20	39.22	27.52	-
V ₂ O ₅ CPC40	28.93	17.23	41°
V ₂ O ₅ CPC60	28.93	17.23	41°
V ₂ O ₅ CPC80	28.01	16.31	38°
V ₂ O ₅ CPC100	33.93	22.23	-

According to interlayer distance of 16.80, 18.70, 17.23 e 16.31 Å, one can point out that CPC molecules (C₂₁H₃₈ClNH₂ = 21.80 Å) are inclined in angle of 40°, 47°, 41° and 38° respectively, in the plane of V₂O₅ and adsorbed on vanadil group surface [21]. This fact can be associated with the possibility of self-assembling of the CPC molecules present after intercalation. In other words, this result indicates that there are different conformations of CPC into the matrix due to the angle inclinations values. In the case which the composites presented a interlayer lower that 21.80 Å the CPC molecules can present the orientation 2 or 3 as showed in Figure 2. In the other hand, for V₂O₅CPC3, V₂O₅CPC20 and V₂O₅CPC100, the interlayer increase is even greater, 28.40, 27.52 and 22.23 Å, indicating a perpendicular formation of CPC into the matrix, as showed the orientation 1 from Figure 2 [22].

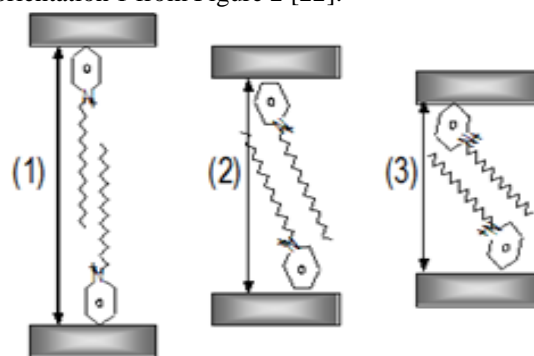


Fig. 2 Scheme of possibilities of CPC orientation between the layers of the matrix: orientation (1), (2) or (3).

However, increasing the surfactant concentration, observed in the increase of CPC aggregate, the adsorption density almost not alters. Kung and Hayes [23] observed the same result and they showed that vibrational energy from CPC adsorbed is the same in different concentration of CPC and the increase of this concentration results in perpendicular conformation in two layers, i.e., a bilayer (Figure 2, orientation 1). Then, it is possible to assume that the increase of interlayer distance is

not, necessary, influenced only with the concentration of guest species (Figure 3) but with the adsorption density of the matrix.

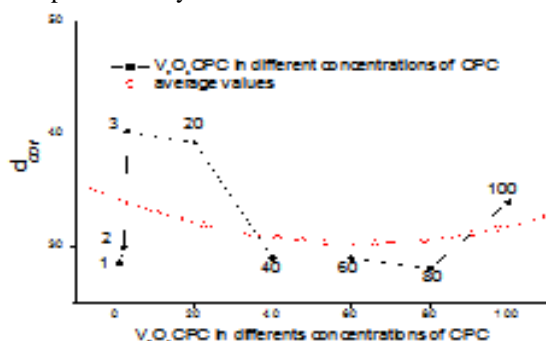


Fig. 3 Distance basal values, d_{001} , in function of V_2O_5/CPC in different concentration of CPC

Furthermore, the interplanar distance of the matrix decreased from 27.52 Å to 17.23 Å when the concentration increased from 20 to 40 mmol/L. In higher concentrations of CPC (above 40 mmol/L), it was observed a decrease of interlayer distance until 80 mmol/L of CPC and, finally, an increase in 100 mmol/L. This behavior can be due to higher concentration of surfactant molecules located around the matrix and not totally into the into the layers. Therefore, from the results obtained, it was observed that the increase in basal spacing of the matrix is, at most, 28.40 Å for $V_2O_5/CPC3$ composite.

In addition, at the diffractograms can be observed that the insertion of CPC promoted the formation of two phases or domains on the same intercalation compound, that is represented by the reflection peaks 001 and 001' and shown in Table 2. This important observation may indicate that the molecules of CPC may, at this stage, reorganize intermittently, thus forming two domains within the matrix.

Table 2 Indication of domain presents in the composites based on X-Ray diffraction pattern results.

	Domain I	Domain II	Domain I	Domain II	Domain I	Domain I and II	Domain I	Domain II
$V_2O_5/CPC1$ (θ)	28.50	13.24						
$V_2O_5/CPC2$ (θ)	29.91	20.47	14.26	10.18			7.21	
$V_2O_5/CPC3$ (θ)	40.10	29.37	19.39	14.28		10.09	8.01	7.14
$V_2O_5/CPC20$ (θ)	39.22	29.81	20.10	14.42		9.55		7.13
$V_2O_5/CPC40$ (θ)	28.93	20.05	14.42			9.54		7.13
$V_2O_5/CPC60$ (θ)	28.93	19.65	14.28			9.54		7.13
$V_2O_5/CPC80$ (θ)	28.01	20.05	14.28			9.44		7.13
$V_2O_5/CPC100$ (θ)	33.93	28.93	16.87	14.42		11.16	8.33	7.46

Although all solutions containing CPC prepared in obtaining composites were above the critical micellar constant ($CMC = 9 \times 10^{-4} \text{ mol dm}^{-3}$) [24],

spherical formation micelles along the plane of the matrix were not observed, since the spherical micelle has a diameter about 45 Å and it only depends on the orientation of the adsorption density.

The peaks observed in the diffractogram also indicated that the compounds were formed with lower crystallinity compared with the X-ray diffraction pattern of the matrix. Observing only the crystallinity of composites (Figure 1 b-i), it was noted a larger and lower intensity peak for the $V_2O_5/CPC1$ (Figure 1 (d)) and, with increasing of surfactant concentration, the crystallinity is also increased. In addition, the occurrence of different domain of surfactant after the intercalation reaction provides a greater disassemble of the layer along the matrix. That is, the appearance of peaks at 2θ angles of 4.30° to the composites, (Figure 1 (b) and (i)) may indicate that there was a modification of the aggregates of surfactant while increasing its concentration and, thus, forming a new phase arranged inside the layers (Table 2) as also observed in literature [25].

Figure 4 (a-c) shows the FTIR spectra of the matrix, CPC and composite $V_2O_5/CPC3$. In this spectrum can be observed the bands corresponding to the matrix: 1010 cm^{-1} - $\nu(V=O)$; 763 cm^{-1} - $\nu(VOV)$; 511 cm^{-1} - $\delta(VOV)$, as well as surfactants and the $V_2O_5/CPC3$ composite corresponding to: $\nu(NH)$ - 3450 cm^{-1} ; $\nu(CH)$ - 2840 cm^{-1} ; $\nu(C=C)$ and $\nu(CN)$ - 1640 cm^{-1} and 1470 cm^{-1} , $\nu(CH_2)$ - 1320 cm^{-1} . After the intercalation reaction was observed in the spectrum (Figure 4c) displacement of the band corresponding to the vibration of $\nu(V=O)$. This shift can occur, probably due to the occurrence of electrostatic interactions between the positive charges of the surfactant in contact with the negative charge density of VO bond. Beyond to the electrostatic interactions, it is assumed that the CP^+ molecules may have other interactions such as hydrophobic cooperative interactions between the aromatic rings pyridinium linked in the surface of the oxide, as well as $\pi-\pi$ interactions between neighboring rings pyridinium [26]. The spectra of the others composites presented similar bands to those shown in Figure 4 (c).

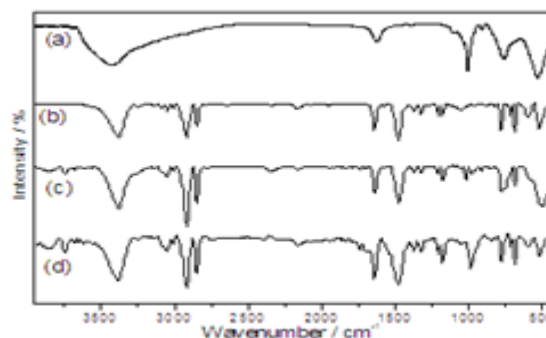


Fig. 4 FTIR spectra of (a) V_2O_5 xerogel, (b) CPC, (c) $V_2O_5/CPC3$ e $V_2O_5/CPC40$.

Figure 5 shows the images of scanning electron microscopy of the matrix and composites V_2O_5 CPC. For the SEM image of V_2O_5 xerogel, is possible to note the presence of interconnected fibers with a thickness of around 50 nm, forming a non-homogeneous texture. With the addition of surfactant was observed a modification on the surface of the composites. More specifically, after insertion of the surfactant was observed that the fibers along the surface showed a greater thickness as compared with the matrix. The micrograph of the V_2O_5 CPC1 composite showed a surface with the formation of fibers with a thickness of around 3000 nm, thus being a very rough surface.

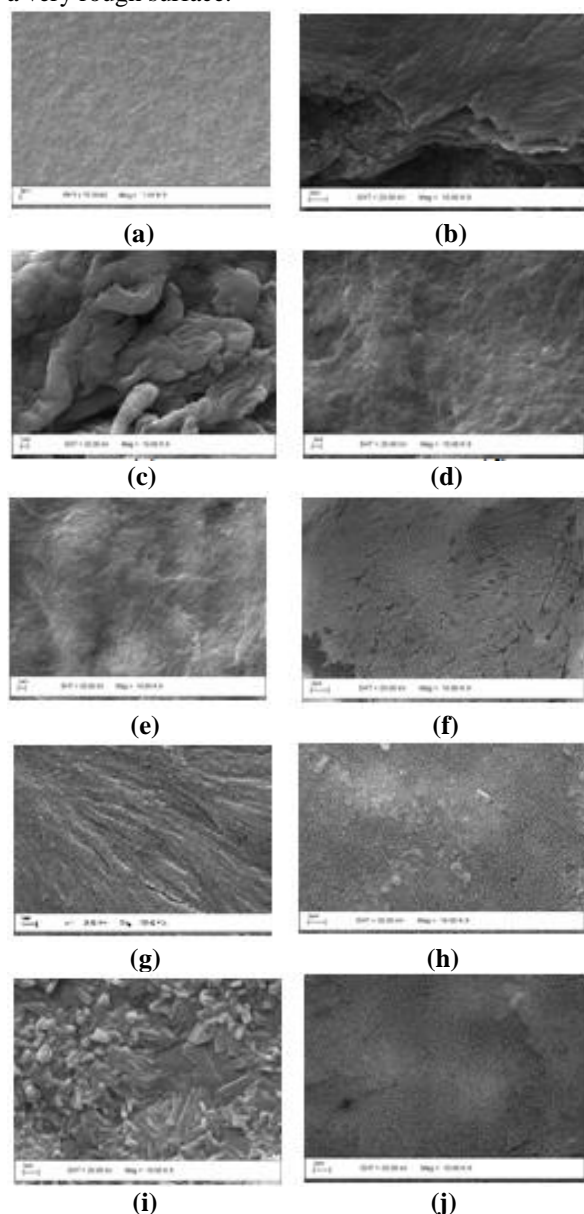


Fig. 5 Scanning electron micrographs of (a) V_2O_5 xerogel, (b) V_2O_5 CPC40 in side view, (c) V_2O_5 CPC1, (d) V_2O_5 CPC2, (e) V_2O_5 CPC3, (f) V_2O_5 CPC20, (g) V_2O_5 CPC40, (h) V_2O_5 CPC60, (i) V_2O_5 CPC80 and (j) V_2O_5 CPC (10.000 x).

However, as increased the amount of surfactant, such as V_2O_5 CPC2 and V_2O_5 CPC3, the structure presented a formation of fiber with thickness of about 100 nm, smaller than the V_2O_5 CPC1 as well as, became more homogeneous the along the surface and, consequently, a higher crystallinity compared to V_2O_5 CPC1.

The thickness of the fibers along the surface of the material decreases with increasing concentration of CPC in the intercalation compounds. However, in the micrographs of V_2O_5 CPC60 and V_2O_5 CPC80 composite (Figure 5 (h-i)), despite having a smooth surface, there was observed the formation of rod-shaped pellet with a thickness of about 500 nm within the material. Further, the composites V_2O_5 CPC20, V_2O_5 CPC40 and V_2O_5 CPC100 micrographs showed the formation of a rough surface with pellets having a diameter around 180 nm. The change of the surface of the composite V_2O_5 CPC100 may be related to excess of CPC not intercalated in the matrix.

IV. CONCLUSIONS

The synthesis, structural properties of vanadium pentoxide xerogel–CPC hybrid materials have been described. The V_2O_5 CPC composites materials presented a lamellar structure and a different phase and domain for different concentration of surfactant. Although narrowing of the X-ray line suggests there is an increase in the layer stacking order even in different conformation of CPC into the matrix. The decrease of interlayer distance from 20 mmol/L to 100 mmol/L can be due to the surfactant molecules located around the matrix and not totally into the into the layers. Further, these materials will be tested, after thermal treatment, as porous materials to be applied as cathode in for lithium ions batteries.

V. ACKNOWLEDGEMENTS

The authors gratefully acknowledge the fellowship provided by CAPES, FAPESP, FAPEMIG, INEO and CNPq are also acknowledged for financial support.

REFERENCES

- [1] G. Huan, A.J. Jacobson, J.W. Johnson and E.W. Corcoran, *Hydrothermal synthesis and single-crystal structural characterization of the layered vanadium(IV) phosphate $VOC_6H_5PO_3 \cdot nH_2O$* , *Chemical Materials*, 2, 1990, 91-93.
- [2] J.W. Johnson, J.F. Brody and R.M. Alexander, *Vanadyl benzylphosphonates and vanadyl naphthylphosphonates: intercalation reactions with butanols*, *Chemical Materials*, 2, 1990, 198-201.
- [3] Y-C. Liao, Y-C. Jiang and S-L. Wang, *Discrete Water Hexamers and Template-Assisted Molecular Recognition in an Elastic*

- Zincophosphate Lattice, *Journal of American Chemical Society*, 127, 2005, 12794-12795.
- [4] Y-C. Liao, C-H Lin and S-L Wang, *Direct White Light Phosphor: A Porous Zinc Gallophosphate with Tunable Yellow-to-White Luminescence*, *Journal of American Chemical Society*, 127, 2005, 9986-9987.
- [5] Y-C. Yang, L-I. Hung and S-L. Wang, *New Series of Layered Vanadyl Phosphates with Varied Polyamine Templates*, *Chemical Materials*, 17, 2005, 2833-2840.
- [6] A. Clearfield and Z. Wang, *Organically pillared microporous zirconium phosphonates*, *Journal of Chemical Society*, 15, 2002, 2937-2947.
- [7] A.D. Wadsley, *The crystal structure of $Na_{2-x}V_6O_{15}$* , *Acta Crystallographica*, 8, 1955, 695-701.
- [8] K. Nielsen, R. Fehrmann and K.M. Eriksen, *Crystal structure of cesium (.mu.-oxo) bis (oxodisulfatovanadate) $Cs_4(VO)_{20}(SO_4)_4$* , *Inorganic Chemistry*, 32, 1993, 4825-4828.
- [9] Y. Oka, F. Saito, T. Yao and N. Yamamoto, *Crystal Structure of $Cs_2V_4O_{11}$ with Unusual V-O Coordinations*, *Journal of Solid State Chemistry*, 134, 1997, 52-58.
- [10] M.S. Whittingham and A.J. Jacobson, *Intercalation Chemistry* (Academic Press, New York, 1982).
- [11] J.M. Reinoso, H.J. Muhr, F. Krumeich, F. Bieri and R. Nesper. *Controlled Uptake and Release of Metal Cations by Vanadium Oxide Nanotubes*, *Helvetica Chimica Acta*, 83, 2000, 1724-1733.
- [12] H.Y. Kang, L.M. Meyer, R.C. Haushalter, A.L. Schweitzer, L. Zubieta and J.L. Dye, *Giant Voids in the Hydrothermally Synthesized Microporous Square Pyramidal-Tetrahedral Framework Vanadium Phosphates $[HN(CH_2CH_2)_3NH] K_{1.35}[V_5O_9(PO_4)_2] \cdot xH_2O$ and $Cs_3[V_5O_9(PO_4)_2] \cdot xH_2O$* , *Chemical Materials*, 8, 1996, 43-53.
- [13] Y. Zhang, C.J. Warren and R.C. Haushalter, *Comparative Study of the Structural, Electronic, and Magnetic Properties of the Layered Ternary Vanadium Oxides CaV_4O_9 , $Cs_2V_4O_9$, and $[H_2N(CH_2)_4NH_2]V_4O_9$* , *Chemical Materials*, 10, 1998, 1059-1064.
- [14] M.S. Whittingham, *The electrochemical characteristics of VSe₂ in lithium cells*, *Materials Research Bulletin*, 13, 1978, 959-965.
- [15] F. Huguenin and R.M. Torresi, *Electrochemical Behavior and Structural Changes of V₂O₅ Xerogel*, *Journal of Brazilian Chemical Society*, 14, 2003, 536-543.
- [16] E.M. Guerra, D.T. Cestarolli, L.M. Da Silva and H.P. Oliveira, *Synthesis, characterization and electrochemical behavior of the vanadium pentoxide/cetyl pyridinium chloride hybrid material* *Journal of Solid State Electrochemistry*, 14, 2010, 305-312.
- [17] G.D. Stucky, A. Monnier, F. Schiith, Q. Huo, D. Kumar, D. Margolese, M. Krishnamurty, P. Petroff, A. Firouzi, M. Janicke and B.F. Chmelka, *Molecular and Atomic Arrays in Nano- and Mesoporous Materials Synthesis*, *Molecular Crystals and Liquid Crystals*, 240, 1994, 187-200.
- [18] M. Wiebcke, M. Grube, H. Koller, G. Engelhardt and J. Felsche, *Structural links between zeolite-type and clathrate hydrate-type materials: Redetermination of the crystal structure of $[N(CH_3)_4]_8[Si_8O_{20}] \cdot 65 H_2O$ by single-crystal X-ray diffraction and variable-temperature MAS NMR spectroscopy*, *Microporous Materials*, 2, 1993, 55-63.
- [19] Z.S. Chao and E. Ruckenstein, *Phase Behavior of Mesoporous V-Mg-O*, *Langmuir*, 19, 2003, 4235-4245.
- [20] E.M. Guerra, K.F. Ciuffi and H.P. Oliveira, *V₂O₅ xerogel-poly(ethylene oxide) hybrid material: Synthesis, characterization, and electrochemical properties*, *Journal of Solid State Chemistry* 179, 2006, 3814-3823.
- [21] F. Carn, N. Steunou, L. Livage, A. Colin and R. Backov, *Macroporous Vanadium Oxide Foams*, *Chemical Materials*, 17, 2005, 644-649.
- [22] A.A. El-Meligi, *Synthesizing layered material of FePS₃ and its intercalation with pyridinum*, *Materials Chemistry and Physics*, 89, 2005, 253-259.
- [23] K-H.S. Kung and K.F. Hayes, *Fourier transform infrared spectroscopic study of the adsorption of cetyltrimethylammonium bromide and cetylpyridinium chloride on silica*, *Langmuir*, 9, 1993, 263-267.
- [24] O.E. Philippova, L.A. Chtcheglova, N.S. Karybians and A.R. Khokhlov, *Two mechanisms of gel/surfactant binding*, *Polymer Gels and Networks*, 6, 1998, 409-421.
- [25] P.M. Lindemuth and G.L. Bertrand, *Calorimetric observations of the transition of spherical to rodlike micelles with solubilized organic additives*, *Journal of Physical Chemistry*, 97, 1993, 7769-7773.
- [26] P. Praus, M. Turicová, S. Študentová and M. Ritz, *Study of cetyltrimethylammonium and cetylpyridinium adsorption on montmorillonite*, *Colloid and Interface Science*, 304, 2006, 29-36.